BULLETIN DE L'ASSOCIATION MINÉRALOGIQUE DU CANADA

THE CANADIAN MINERALOGIST

JOURNAL OF THE MINERALOGICAL ASSOCIATION OF CANADA

Volume 41 October 2003 Part 5

The Canadian Mineralogist
Vol. 41, pp. 1105-1124 (2003)

HYPOGENE TITANIAN, VANADIAN MAGHEMITE IN REWORKED OXIDE CUMULATES IN THE BEJA LAYERED GABBRO COMPLEX, ODIVELAS, SOUTHEASTERN PORTUGAL

ANA P. JESUS§

CREMINER, Faculdade de Ciências, Universidade de Lisboa, Ed. C2, Piso 5, Campo Grande, 1749 016 Lisboa , Portugal

ANTÓNIO MATEUS

Departamento de Geologia and CREMINER, Faculdade de Ciências, Universidade de Lisboa, Ed. C2, Piso 5, Campo Grande, 1749-016 Lisboa , Portugal

JOÃO C. WAERENBORGH

Departamento de Química, Instituto Tecnológico e Nuclear, 2686-953 Sacavém, Portugal

JORGE FIGUEIRAS

Departamento de Geologia and CREMINER, Faculdade de Ciências, Universidade de Lisboa, Ed. C2, Piso 5, Campo Grande, 1749-016 Lisboa, Portugal

LUÍS CERQUEIRA ALVES

Dep. Física, Instituto Tecnológico e Nuclear, 2686-953 Sacavém, Portugal

VITOR OLIVEIRA

Instituto Geológico e Mineiro, Rua Frei Amador Arrais, 39 r/c, Apartado 104, 7802 Beja Codex, Portugal

ABSTRACT

At Odivelas (Beja, Portugal), massive accumulations of coarse-grained magnetic oxides occur within the lower group of a layered, synorogenic Variscan gabbroic sequence. These oxide bodies, irregular in shape, at approximately right angles to the regional layering and of considerable size (up to an estimated 50 t each), are mainly composed of vanadium-bearing titanian maghemite, as large equant grains forming a polygonal texture, poikilitic ilmenite and accessory amounts of maghemite. No Fe^{2+} was detected by Mössbauer spectroscopy in either maghemite and titanian maghemite. Strongly weathered samples show hematite

§ *E-mail address*: ana.jesus@fc.ul.pt

and goethite replacing the maghemite or forming late veinlets cutting all oxide phases. Apart from these supergene veinlets, no fracturing is discernible within the oxide bodies; also, no zonation was found in the oxide phases, despite an examination by several techniques (reflected light microscopy, EPMA and micro-PIXE). The irregular and discordant shape of these bodies must have resulted from localized settling of primary oxide grains in the magma chamber or from gravitational destabilization of previously formed layers of oxide minerals. A supergene origin for these accumulations of maghemite is discounted because of textural considerations and the total absence of hydrous alteration. The surrounding gabbroic rocks show no alteration and host an oxide assemblage composed of titanian magnetite and ilmenite, which closed chemically at around 650–675°C, thus above the experimental threshold for maghemite formation. The oxide bodies of Odivelas thus underwent an oxidation process that has not affected their host rocks and that must have been caused by the focusing to their margins of late degassing fluids owing to rheological contrasts. As soon as the oxidizing fluids reached the oxide accumulations, oxidation proceeded by intergranular diffusion until all primary spinels were converted to maghemite, but did not spread to the country rocks, owing to the sluggishness of diffusion through silicates at these temperatures. The development of part of the observed ilmenite and of the precursor of Ti-free maghemite seems to result from the early stages of the oxidation process, according to the equation normally describing oxidation-induced exsolution in titanian magnetite. The ilmenite and spinel structures remained intact under further strong oxidation, probably owing to the incorporation of minor cations inherited from the original spinel.

Keywords: titanian maghemite, oxidation, layered gabbros, Mössbauer spectroscopy, micro-PIXE, Beja Igneous Complex, Portugal.

Sommaire

Nous décrivons, à Odivelas, dans la région de Beja, au Portugal, des accumulations massives d'oxydes magnétiques à gros grains dans la partie inférieure d'une séquence gabbroïque stratiforme d'âge varisque. Ces amas d'oxydes, de forme irrégulière, disposés environ perpendiculairement au pendage régional et atteignant une taille considérable (une cinquantaine de tonnes chaque), contiennent surtout une maghémite titanifère et vanadifère en grains équidimensionnels polygonaux, entourés d'ilménite poecilitique, avec une maghémite pure comme accessoire. Nous n'avons décelé du Fe^{2+} ni dans la maghémite, ni dans la maghémite titanifère. Dans les échantillons altérés par météorisation, l'hématite et la goethite remplacent la maghémite ou forment des veinules tardives recoupant tous les oxydes. A part ces veinules, nous ne voyons pas de fractures dans ces amas d'oxydes; de plus, nous ne voyons pas de zonation dans les oxydes, malgré un examen minutieux avec plusieurs techniques (microscopie en lumière réfléchie, analyses à la microsonde électronique, analyses micro-PIXE). La forme irrégulière et discordante de ces amas résulterait d'abord d'une accumulation de grains d'oxydes dans la chambre magmatique, les cumulats d'oxydes étant possiblement déstabilisés sur une pente. Une origine supergène de ces accumulations de maghémite semble peu probable compte tenu des textures et de l'absence totale de produits hydratés d'altération. Les roches gabbroïques avoisinantes ne montrent aucun signe d'altération, et contiennent un assemblage habituel de magnétite titanifère et d'ilménite, les paires devenant des systèmes fermés à environ 650–675°C, et donc à des conditions supérieures au seuil de formation de la maghémite. Les amas d'oxydes à Odivelas ont donc subi un processus d'oxydation qui n'a pas affecté leurs roches hôtes, et qui a dû impliquer de façon localisée (à cause d'un contraste rhéologique) un flux d'une phase fluide formée par dégazage. Aussitôt que la phase fluide oxydante eut atteint les amas d'oxydes, l'oxydation a procédé par diffusion intergranulaire jusqu'à la transformation complète du spinelle primaire en maghémite, mais sans interaction avec les roches-hôtes, à cause de la lenteur de la diffusion au travers des silicates à ces températures. Le développement d'une partie de l'ilménite observée et du précurseur de la maghémite dépourvue de Ti semble hérité des stades précoces du processus d'oxydation, selon l'équation normalement utilisée pour expliquer l'exsolution provoquée par l'oxydation de la magnétite titanifère. Les structures de l'ilménite et du spinelle sont demeurées intactes au cours de la progression de l'oxydation, probablement à cause de la présence de cations mineurs hérités du spinelle originel.

(Traduit par la Rédaction)

Mots-clés: maghémite titanifère, oxydation, gabbros stratifiés, spectroscopie de Mössbauer, analyse micro-PIXE, complexe igné de Beja, Portugal.

Introduction

Common anorthositic, gabbroic or noritic sequences in plutonic layered complexes commonly comprise massive aggregates of titanian magnetite, with or without ferrian ilmenite, that can form bodies large enough to have been economically exploited [Duchesne (1999), Kärkkäinen & Appelqvist (1999); see also Parsons (1987) and references therein]. The origin of these massive aggregates is somewhat controversial, but should be regarded as part of the magmatic fractionation trend giving rise to their host rocks, as suggested by many experimental results and by the relatively constant mineralogical-textural features observed in such geological systems (Rumble 1976, Frost & Lindsley 1991, Snyder *et al.* 1993, Topplis & Carroll 1995); indeed, the oxide aggregates are almost invariably composed of coarse and equant Ti-bearing spinel grains that commonly display several types of exsolution (usually, lamellae of ulvöspinel or of ilmenite in titanian magnetite), and these grains show trace amounts of vanadium, chromium, aluminum and magnesium. Besides ilmenite,

variable amounts of apatite, rutile and hematite (usually as rims around, or lamellae within, magnetite or ilmenite) are widespread. The majority of these features are compatible with the conclusions inferred from phase-equilibrium relationships among Fe–Ti oxides (Buddington & Lindsley 1964, Frost & Lindsley 1991, Putnis 1992), which show that subsolidus oxidation of magnetite–ulvöspinel with subsequent formation of ilmenite–hematite lamellae takes place during the cooling stages of the magmatic system. Maghemite, on the contrary, is scarce, and generally ascribable to secondary (mostly supergene) alteration of a pre-existing spinel-group mineral.

In this work, massive bodies of Fe–Ti–V oxide occurring at Odivelas, Beja, Portugal, are examined in detail by means of a multidisciplinary approach involving optical petrography, whole-rock geochemistry, electron microprobe and micro-PIXE analysis, powder X-ray diffractometry and Mössbauer spectroscopy. These oxide bodies are hosted by a layered gabbro sequence belonging to the Beja Igneous Complex, and display an uncommon mineral paragenesis, mainly composed of coarse grains of vanadiferous titanian maghemite. After demonstrating the maghemitic character of the Fe–Ti–V spinel and addressing the reasons that support its non-supergene origin, we evaluate the strong subsolidus oxidation that allowed its development.

Geological Setting

The Beja Igneous Complex (BIC) is a wide curvilinear intrusive belt that can be followed for *ca.* 100 km in the westernmost domain of the Ossa–Morena Zone, along the southern border in Portugal (Fig. 1). According to the available data, the emplacement of the BIC results from important synorogenic, Variscan magmatic activity that lasted for over 25–30 Ma, from Frasnian–Famennian (Upper Devonian) to Late Visean times (Lower Carboniferous). This complex intrusive belt can be divided in three prominent units: 1) the Beja Gabbroic Complex, mainly consisting of olivine-bearing gabbroic rocks, rimmed by heterogeneous diorites resulting from variable extents of magma mixing or assimilation of crust, 2) the Cuba–Alvito Complex, comprising mostly granodiorite, diorite and gabbro, and 3) the Baleizão Porphyry Complex, a late, very shallow intrusion embracing various types of porphyry rocks (Andrade 1974, 1983, Perroud *et al.* 1985, Santos 1990, Santos *et al.* 1990, Dallmeyer *et al.* 1993, Quesada *et al.* 1994, Fonseca 1995, Araújo 1995).

In the Odivelas area, the westernmost part of the Beja Gabbroic Complex can be well characterized (Silva *et al.* 1970, Andrade 1983, Santos *et al.* 1990). Detailed geological mapping of this area, complemented by petrographic and geochemical studies (Jesus 2002), reveals that the outcropping rocks are quite diverse and generally layered, forming two main series that show normal polarity; they come in contact with one another along a narrow (~5 m) belt where the distinctive features of one of the series fade continuously while the features characteristic of the other series appear gradually (Fig. 2). The lower magmatic sequence, labeled as Series I, consists of three main groups of layers. The lower group comprises essentially olivine leucogabbro, within which layers and lenses (blocks?) of troctolitic rocks and of oxide-rich cumulates (olivine melagabbro, wehrlite and websterite) can be identified, besides irregular bodies of massive, magnetic Fe–Ti–V oxide aggregates. The intermediate group of Series I is mostly composed of leucogabbro and anorthosite, and the upper group consists of a relatively monotonous sequence of olivine leucogabbro that contains discontinuous lenses of anorthosite. In Series I, the layering is not uniformly developed, and may be difficult to distinguish, particularly within several domains of the lower group; nevertheless, far from major fault zones, the dip of the layer is relatively constant regardless of the rock type (<30° SSW or SW), ranging in strike from NW–SE to WNW–ESE. The basal domains of the upper magmatic sequence (Series II) are mainly composed of almost massive olivine gabbro; the overlying olivine leucogabbro forms a relatively thick packet in which successions of distinct compositional layers (including a few of anorthositic nature) are observed to repeat rhythmically. In Series II, the strike of the layers ranges between WNW–ESE and E–W, and its dip is less than 30° SSW or S.

Considering the modal cyclicity usually observed in the Odivelas area, along with the cryptic layering well preserved in some gabbroic sequences (Jesus 2002), the series described above are interpreted as megacyclic units, as defined by Irvine (1987). In addition, the available data suggest that the mechanisms responsible for layer development are mainly due to non-dynamic processes (in the sense of Boudreau & McBirney 1997, McBirney & Nicolas 1997), but that all rock types have accommodated significant strain during their crystallization.

As referred to above, the irregular bodies of massive, magnetic Fe–Ti–V oxide aggregates (up to 50 tonnes each, according to the estimates of the exploration surveys performed in 1944: Silva 1945) are confined to the lower group of Series I, and are hosted by gabbroic domains significantly enriched in interstitial titanian magnetite and ilmenite. However, the field relationships between the oxide masses and their host rocks are poorly known because the contacts cannot be observed owing to extensive agricultural activity (Jesus 2002). Note that the nearest outcrops of gabbroic rocks in the vicinity of the oxide bodies are located up to 100 m away from them. These accumulations of oxide may have economic interest, as recently discussed by Mateus *et al.* (2001) on the basis of the studies carried out by Fonseca (1999) and by Gonçalves *et al.* (2001), who evaluated the available geophysical and soil geochem-

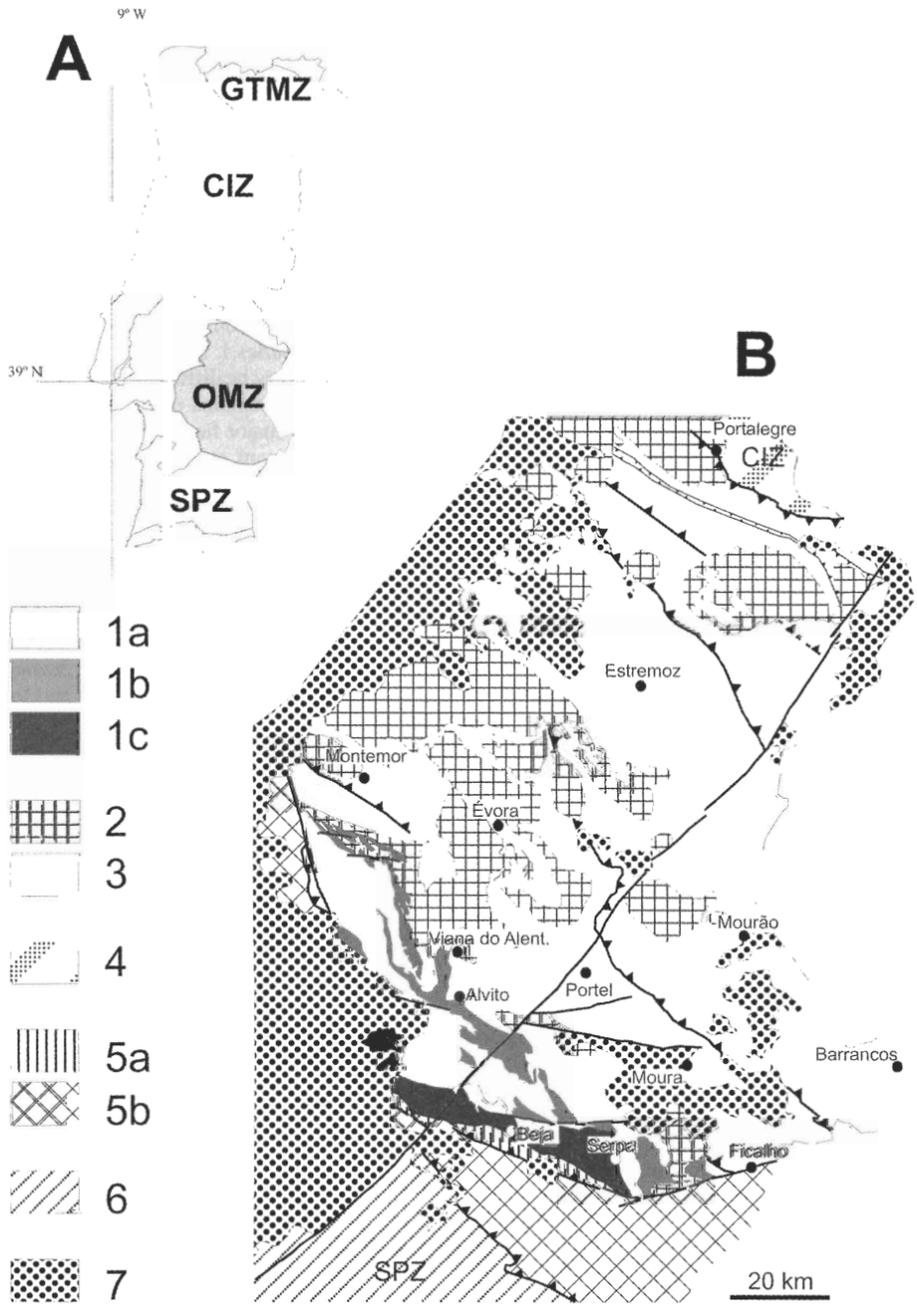

FIG. 1. A. Major geotectonic units of southwestern Iberia. CIZ: Central Iberian Zone, GTMZ: Galicia – Trás-os-Montes Zone, OMZ: Ossa–Morena Zone, SPZ: South Portuguese Zone. B. Schematic geological map of the OMZ: 1) Beja Igneous Complex, a) Baleizão Porphyry Complex, b) Cuba–Alvito Complex, c) Beja Gabbroic Complex. 2) Undifferentiated Variscan Granitoid rocks. 3) Undifferentiated metasedimentary and metavolcanic sequences and ultramafic rocks. 4) Metasedimentary rocks of CIZ. 5) Oceanic exotic terranes, a) Beja–Acebuches Ophiolite Complex, b) Pulo do Lobo Group (metasedimentary and metavolcanic units). 6) Metasedimentary and metavolcanic sequences of SPZ. 7) Cenozoic sedimentary cover.

FIG. 2. Geological map of the Odivelas area (after Mateus *et al.* 2001, Jesus 2002). 1) Cenozoic detrital sediments. 2) Late diorite intrusive bodies. Series II: 3) olivine gabbro, 4) olivine leucogabbro. Upper Group of Series I: 5) anorthosite, 6) olivine leucogabbro. Intermediate Group of Series I: 7) anorthosite, 8) leucogabbro. Lower Group of Series I: 9) olivine leucogabbro, 10) oxide-rich cumulates, 11) bodies of massive Fe–Ti–V oxide. 12) Amphibolitized and chloritized rock domains (chiefly controlled by major fault-zones). 13) Geological contacts. 14) Inferred fault-zone. 15) Fault zone. 16) Magmatic layering. 17) Foliation.

istry data, respectively. The results obtained show that the magnetic anomalies are not limited to the small area surveyed for iron ores in 1944 (Silva 1945), and that the mineralized bodies are quite enriched in titanium and vanadium (up to 10.05 wt% of TiO_2 and up to 0.99 wt% of V_2O_5). No accurate estimates of reserves are presently available.

Analytical Methods

After petrography, chemical analyses were conducted on representative polished thin sections using a three-channel wavelength-dispersion JEOL–JCXA 733 electron microprobe, operated at an accelerating voltage of 18 kV and a beam current intensity of 25 nA. Natural mineral and pure metal (V) standards were analyzed before, during and after each analytical session; the estimated error associated with the values obtained is less than 2%.

The same polished thin sections were used in micro-PIXE analysis. For these experiments, an Oxford Microbeams® nuclear-microprobe-type set-up (Alves *et al.* 2000) was used to focus a 2 MeV proton beam generated with a Van de Graaff accelerator. X-ray spectra were accumulated with an 80 mm^2 Si(Li) detector and 155 eV resolution located at a backward angle of 45° and at a distance of 25 mm from the sample. The spatial resolution of the beam was initially set to 3 μm, with a beam current close to 200 pA. The focused beam was raster-scanned over some previously defined regions of interest of the samples, and two-dimensional X-ray elemental maps were obtained. From those maps, some spots were chosen to perform micro-PIXE point analysis. Basic acquisition and manipulation of data and mapping were done with the OM–DAQ program (Grime & Dawson 1995), whereas spectra fitting and quantitative results were obtained with the GUPIX computer package (Maxwell *et al.* 1995), which accounts for matrix and secondary fluorescence corrections.

The samples were crushed cautiously (coarse fragments obtained with an hydraulic rock-crusher were wrapped in paper and then smashed with a hammer to a grain size of 1–2 mm) and prepared separately for whole-rock chemical analysis, X-ray diffraction (XRD) and Mössbauer spectroscopy.

Multi-element chemical analyses were accomplished at the Activation Laboratories Ltd. (Canada) after fine grinding of the samples in a tungsten carbide mill; solutions for ICP–MS and INAA determinations were obtained by acid total digestion, and the FeO and Fe_2O_3 contents were determined by titration. Similar fine powders, spread on silicon plates (Philips PW 1817/32), were used to obtain XRD patterns with a Philips PW 1710 powder diffractometer using Cu$K\alpha$ radiation, a curved graphite crystal monochromator and a PW1820 Bragg–Brentano goniometer; subsequent phase identification was based on the Mineral Powder Diffraction File Databook (Bayliss *et al.* 1993).

The presence of a large number of Fe-containing phases may seriously hinder the interpretation of ^{57}Fe Mössbauer spectra. In cases where both hematite and magnetite or maghemite are present, it is difficult to characterize these oxides even if the whole range in temperature from 293 to 6 K is scanned. In order to separate the grains with the highest magnetic susceptibility, the 1–2 mm grain-size concentrates were broken in a cylinder rock-crusher and sieved. The physical separation of grains using a hand magnet was performed on the 63 μm < ϕ < 90 μm size fraction with the grains immersed in ethanol in order to prevent grain aggregation. Two fractions were thus obtained, HMag, composed of grains with higher magnetic susceptibility (including all grains of the spinel), and the remaining grains, designated as fraction LMag. ^{57}Fe Mössbauer spectra of both HMag and LMag powdered samples were obtained in transmission mode using a conventional constant-acceleration spectrometer and a 25 mCi ^{57}Co source in Rh matrix. The velocity scale was calibrated using an α-Fe foil at room temperature. Spectra were obtained at various temperatures between 293 K and 5 K. Low-temperature measurements were performed using a liquid helium flow cryostat. Absorbers were prepared by pressing the sample powders (≈ 5 mg of natural Fe / cm^2) into perspex holders. The spectra were fitted to Lorentzian peaks using a non-linear least-squares computer method (Waerenborgh *et al.* 1994). The widths and relative areas of both peaks in each quadrupole doublet and of peaks 1–6, 2–5 and 3–4 in each magnetic sextet were constrained to be equal.

Results

Petrography

The massive oxide bodies are composed mostly of a matrix of coarse (5–10 mm), equant and quasi-polygonal Ti-rich spinel grains (A–Spl) enclosing lesser ilmenite that forms centimetric oikocrysts (Fig. 3A). Accessory amounts of a second type of spinel (B–Spl) can also be recognized, occurring widely as small grains (< 1 mm) near the junctions of A–Spl domains (Fig. 3B). The grains of A–Spl are optically homogeneous and do not show oxidation-induced exsolution. Ilmenite grains, containing rare exsolved lamellae of hematite, commonly display a strong pinkish tint. Grains of B–Spl, presenting a mild brownish tint, exhibit a lower reflectance and a greater hardness (as suggested by differences in polishing relief) in comparison to the adjoining A–Spl spinel matrix; they represent indeed a distinct spinel-phase (impoverished in Ti), as will be later discussed.

Samples exposed to strong weathering show evidence of a mineral-textural transformation resulting from replacement along fractures of pre-existing spinel, *i.e.*, both A–Spl and B–Spl, by finely divided hematite (Fig. 3C), besides late fracture infillings by goethite–hematite (Fig. 3D). Occasionally, micropores and late

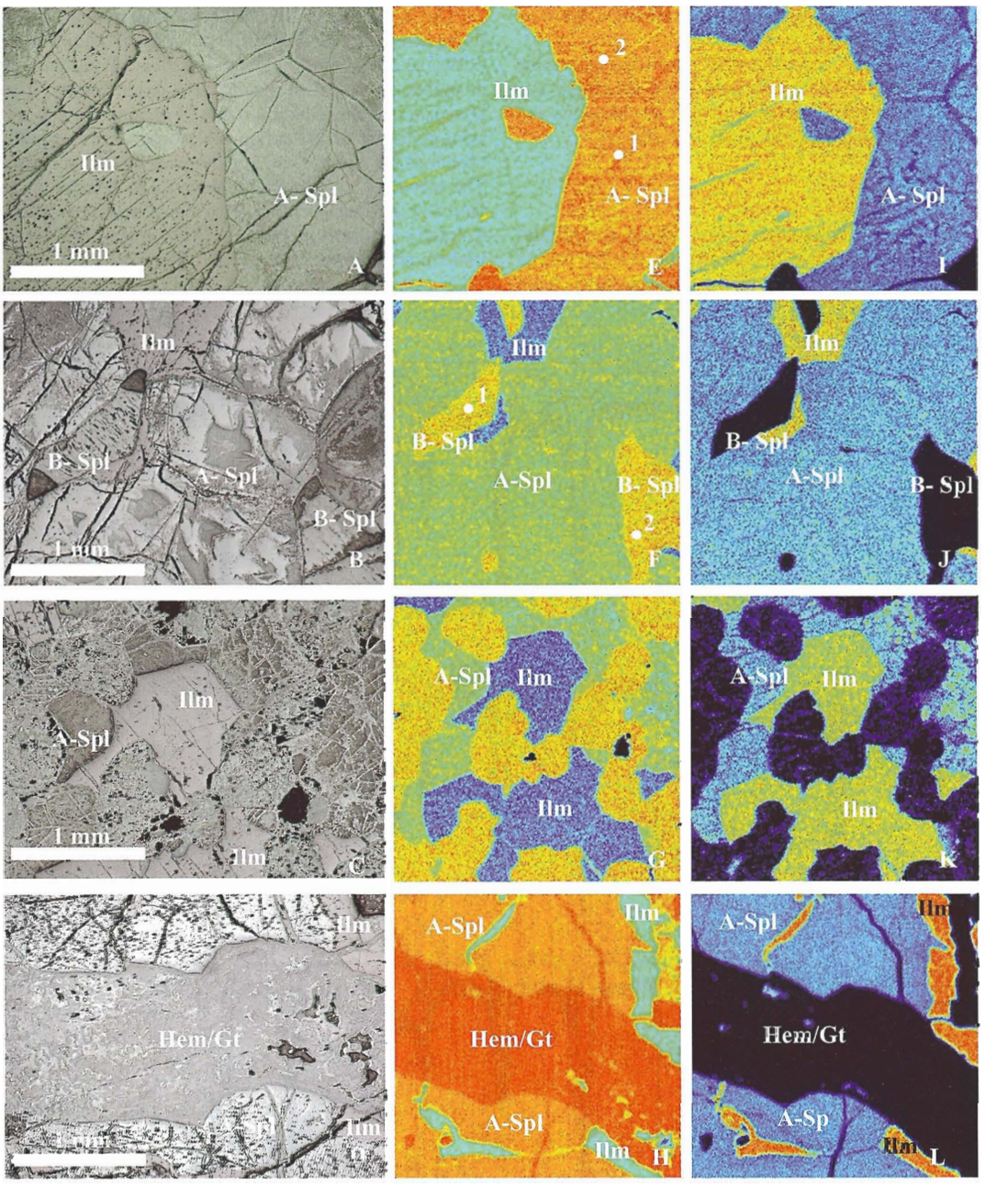

FIG. 3. A. Typical textural relationships shown by the aggregates of massive oxides (matrix titanian maghemite, A–Spl, and poikilitic ilmenite, Ilm). B. Typical textural relationships of Ti-poor spinel (B–Spl). C. Late replacements by hematite along fractures. D. Late hematite–goethite fracture infillings (Hem–Gt). E, F, G, H: Fe-distribution maps obtained by micro-PIXE analysis of the areas corresponding to photos A, B, C and D, respectively. I, J, K, L: Ti-distribution maps obtained by micro-PIXE analysis of the areas corresponding to photos A, B, C and D, respectively. All micro-PIXE elemental maps were obtained from a 2640 × 2640 μm^2 scan; white dots in E and F represent the spots selected for micro-PIXE point analysis.

fractures are filled by aggregates of carbonate that may coexist with goethite.

Typical modal proportions of these massive oxide aggregates are 73–81% of spinel-group minerals, 10–22% of ilmenite, and less than 15% of late hematite and goethite. No other mineral phases are present.

XRD analysis

Powder-diffraction results of representative samples show good agreement with petrographic data, revealing typically ilmenite and (titanian) maghemite as the main mineral phases.

The XRD data of the HMag fraction were analyzed by the Rietveld powder profile program of Young *et al.* (1995) to obtain an estimate of the unit-cell parameters of spinels included in the massive oxide bodies. The presence of spinels with a range of chemical compositions gives rise to diffraction peaks broader than usually observed for phases with a homogeneous composition. The estimated unit-cell parameter, 8.336 ± 0.001 Å, is therefore an average value. This value, however, points to totally oxidized maghemite (Waychunas 1991) and titanian maghemite (Allan *et al.* 1989).

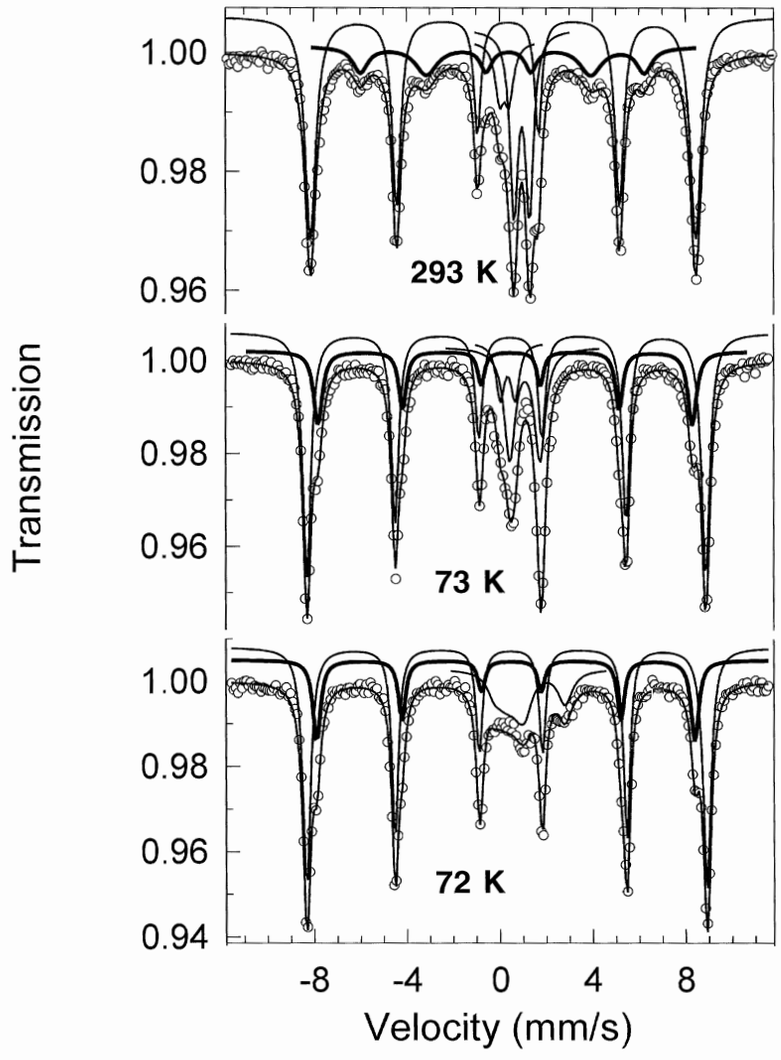

FIG. 4. Mössbauer spectra of the LMag fraction taken at various temperatures. The sextet with the largest splitting is attributed to hematite. The sextet drawn with a thicker line is attributed to goethite. The other subspectra are assigned to ilmenite.

Mössbauer spectroscopy

The 293 K Mössbauer spectrum of LMag (Fig. 4) can be fitted with two magnetic sextets and two quadrupole doublets. The estimated parameters for the sextet, with sharp well-defined lines (Table 1), are typical of hematite. The second sextet, with lower magnetic splitting and broad peaks, is attributed to goethite (Bowen *et al.* 1993). The quadrupole doublet with higher isomer shift, δ, is due to Fe^{2+} in ilmenite, and the remaining doublet, to Fe^{3+}. As the temperature at which the spectra were taken decreases, a gradual sharpening of the peaks and an increase in magnetic splitting of the goethite sextet are observed (Fig. 4). The paramagnetic doublets are still present at 73 K, with no significant changes of the corresponding relative areas, *I* (Table 1), but at 12 K, below the magnetic ordering temperature of ilmenite, they are replaced by the characteristic magnetic splitting of this oxide (Waerenborgh *et al.* 2002). Considering the estimated relative area *I* (Table 1), the Fe^{3+} doublet observed at 73 K and above and no longer present at 12 K is most probably due to superparamagnetic Fe oxides. Within experimental error, in the fraction LMag, with the lowest magnetic susceptibility, no Fe-containing spinel oxides are observed.

The six-peak pattern observed in the 293 K Mössbauer spectrum of the HMag fraction (Fig. 5) is significantly different from the sextets observed in the LMag spectrum. The estimated parameters of this sextet (Table 1) are similar to those published for both maghemite and titanian maghemite (Allan *et al.* 1989, Bowen *et al.* 1993, Vandenberghe *et al.* 2000). Although Fe cations in these oxides are present in octahedral and tetrahedral sites, the resulting two-sextet pattern is insufficiently resolved because of the near-equality of the corresponding hyperfine parameters: at room temperature, differences in magnetic hyperfine fields, B_{hf}, are lower than 0.4 T, and in δ, less than 0.12 mm/s (Da Costa *et al.* 1995).

Because powder X-ray diffractograms of the HMag sample show small amounts of hematite, the presence of a second sextet with parameters equal to those estimated for hematite in LMag (Table 1) was also considered. Only the corresponding relative area *I* was allowed to vary during the regression analysis, and the final fit was found to improve significantly. The detailed absorption observed around zero-velocity may in part be explained by two quadrupole doublets similar to those of Fe^{2+} and Fe^{3+} in ilmenite (Table 1). However, a very broad absorption centered at ~0.34 mm/s, approximately described by a very broad peak, is necessary to obtain a reasonable fit of the spectrum. This finding suggests the presence of slow-relaxing Fe^{3+} magnetic moments, with relaxation times at 293 K of the same order of magnitude as the observation time in Mössbauer spectroscopy ($\sim 10^{-8}$ s), and may be attributed to the presence of superparamagnetic Fe oxide of variable composition or variable detailed structure, but only the low-temperature spectra, to be discussed below, will allow a better characterization of the phases containing this Fe^{3+}.

As already stated, two doublets attributed to Fe^{3+} and Fe^{2+} in ilmenite (Waerenborgh *et al.* 2002) are observed in the 293 and 73 K spectra. At 12 K, the ilmenite is magnetically ordered, as expected (Table 1).

The most significant feature of the 73 and 12 K spectra of HMag is the disappearance of the broad absorption band near zero velocity (Fig. 5). According to the estimated relative area *I*, Fe^{3+} contributing to this band at 293 K seems at 73 and 12 K to give rise to magnetic sextets. At 73 K, a single such sextet, with $B_{hf} \approx 44.4$ T, is sufficient to fit the spectrum, but at 12 K, two sextets, with $B_{hf} \approx 49.3$ and 45.8 T, are needed (Table 1). On the other hand, the Fe^{3+} contributing to the $\gamma(Fe,Ti)_2O_3$ spinel sextet already observed at 293 K is better described by two sextets with $B_{hf} \approx 53.3$ and 51.7 T at 12 K. All four of these magnetic sextets are attributed

TABLE 1. PARAMETERS ESTIMATED FROM THE MÖSSBAUER SPECTRA OF LMag AND HMag SAMPLES, TAKEN AT VARIOUS TEMPERATURES

T		δ mm/s	Δ mm/s	ε mm/s	B_{hf} T	Γ mm/s	I %
			LMag				
293 K	α Fe_2O_3	0.38	-	-0.21	51.4	0.36	60
	α FeOOH	0.38	-	-0.27	37.9	0.54	17
	Fe^{3+}	0.38	0.42	-	-	0.50	6
	Fe^{2+} in $FeTiO_3$	1.08	0.67	-	-	0.41	16
73 K	α Fe_2O_3	0.49	-	-0.18	53.3	0.38	59
	α FeOOH	0.48	-	-0.24	50.0	0.34	18
	Fe^{3+}	0.46	0.63	-	-	0.43	6
	Fe^{2+} in $FeTiO_3$	1.20	1.30	-	-	0.56	17
12 K	α Fe_2O_3	0.49	-	-0.18	53.5	0.34	63
	α FeOOH	0.49	-	-0.24	50.5	0.36	21
	$FeTiO_3$	1.24	-	1.65	4.7	0.50	16
			HMag				
293 K	α Fe_2O_3	0.38	-	-0.20	51.4	0.30	9
	γ $(Fe,Ti)_2O_3$	0.32	-	0.00	50.3	0.52	70
	Fe^{3+}	0.34	-	-	-	2.15	16
	Fe^{3+} in $FeTiO_3$	0.32	0.65	-	-	0.30	2
	Fe^{2+} in $FeTiO_3$	1.08	0.67	-	-	0.38	3
73 K	α Fe_2O_3	0.49	-	-0.18	53.3	0.36	7
	γ $(Fe,Ti)_2O_3$	0.48	-	0.00	53.3	0.45	35
		0.40	-	-0.01	51.7	0.54	37
		0.43	-	0.00	44.4	0.58	15
	Fe^{3+} in $FeTiO_3$	0.41	0.65	-	-	0.30	2
	Fe^{2+} in $FeTiO_3$	1.19	1.30	-	-	0.74	3
12 K	α Fe_2O_3	0.49	-	-0.18	53.6	0.26	7
	γ $(Fe,Ti)_2O_3$	0.49	-	0.02	53.8	0.43	31
		0.42	-	-0.01	51.7	0.48	41
		0.48	-	0.00	49.3	0.39	6
		0.45	-	0.00	45.8	0.72	11
	$FeTiO_3$	1.24	-	1.65	4.7	0.50	4

δ isomer shift relative to metallic Fe at room temperature; Δ quadrupole splitting measured in the paramagnetic state; $\epsilon = (e^2 V_{zz} Q / 4)(3\cos^2\theta - 1)$. The quadrupole shift is calculated from $(\phi_1 + \phi_6 - \phi_2 - \phi_5)/2$, where ϕ_n is the shift of the *n*th line of the sextet due to quadrupole coupling; B_{hf} is the magnetic hyperfine field. Γ full width at half maximum; I relative areas. Estimated standard deviations are <2% for I, <0.2 T for B_{hf} and <0.02 mm/s for the other parameters.

to $\gamma(Fe,Ti)_2O_3$. They are only an approximate description of the absorption due to the A–Spl and B–Spl (titanian) maghemite, as defined in the petrography section. Experimentally, it seems evident that there is a range of B_{hf} values extending from the characteristic values of pure maghemite, ~53–52 T at 12 K (Bowen *et al.* 1993) down to lower values, 46 T. This range of values may arise from different ranges of size of the small particles or of concentration of impurities, namely Ti, B_{hf} decreasing with both size and departure from the ideal composition. Owing to the strong overlap of all the contributions, it is difficult to attribute each fitted sextet to a definite composition or Fe^{3+} coordination, however.

The δ values estimated for the sextets describing the $\gamma(Fe,Ti)_2O_3$ are all characteristic of Fe^{3+}. They are far lower than published data for δ of high-spin Fe^{2+} in any ionic compound or even for δ of $Fe^{2.5+}$, *i.e.*, δ measured when fast electron hopping occurs between Fe^{2+} and Fe^{3+} in either fresh or oxidized magnetite (Weber &

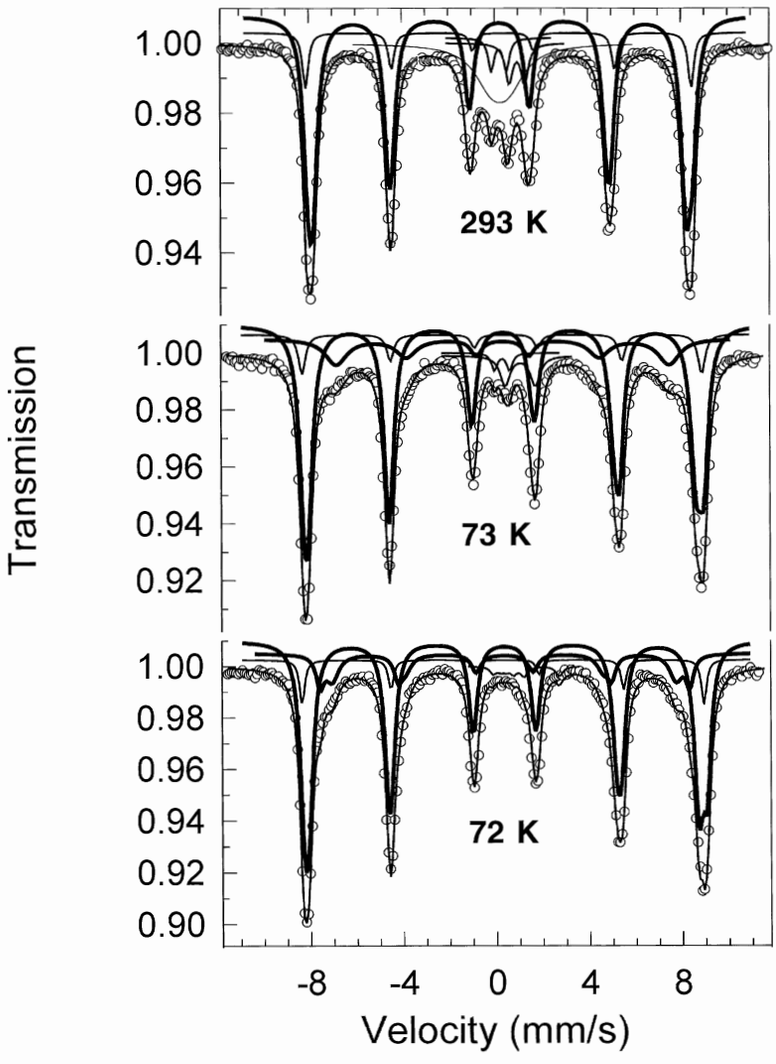

FIG. 5. Mössbauer spectra of the HMag fraction taken at various temperatures. The sextets drawn with a thicker line are attributed to Fe^{3+} in A–Spl and B–Spl. Relaxation effects of a part of this Fe^{3+} give rise to the broad absorption band at 293 K. The sextet observed at all temperatures and drawn with a thinner line is attributed to hematite. The other subspectra are assigned to ilmenite.

Hafner 1971, Ramdani *et al.* 1987, Vandenberghe *et al.* 1998). We therefore conclude that, with the Mössbauer data available, no Fe^{2+} is detected in the spinel-group minerals that form the massive oxide bodies under study.

Electron probe micro-analysis (EPMA)

A total of 36 electron probe micro-analyses were performed on selected samples of the massive oxide bodies. We chose domains of spinel and ilmenite that do not show optical evidence of late alteration or replacement. Representative EPMA results for the spinels (A–Spl and B–Spl types) and for ilmenite, expressed as oxide wt% and normalized cation proportions, are shown in Table 2. All iron in spinels has been taken to be Fe^{3+}, according to the Mössbauer results.

Both A–Spl and B–Spl have relatively uniform chemical compositions, but differ from one another in their Ti contents. The composition of B–Spl is almost pure Fe_2O_3; this spinel must therefore be maghemite. The A–Spl, however, is not a normal titanian maghemite, *i.e.*, a solid solution in Fe_2O_3–Fe_3O_4–$FeTiO_3$–Fe_2TiO_4 space. This is because no divalent (ferrous) cations compensate for the presence of Ti (which may amount to 0.51 atoms per formula unit, *apfu*), leading to a cation distribution that suggests a defect spinel structure, with more vacancies than are present in normal maghemite. The Al and Mg contents are also variable and worth noting, although never exceeding 0.15 Al and 0.10 Mg *apfu* for A–Spl and 0.10 Al and 0.01 Mg *apfu* for B–Spl. The V contents are relatively uniform in A–Spl, varying generally from 0.02 up to 0.04 *apfu*, being much more variable in B–Spl (usually below 0.04, although occasionally it may reach values up to 0.08). Considering all the results, average formulae for A–Spl and B–Spl are $Fe^{3+}_{2.08}Ti_{0.35}V_{0.04}Al_{0.06}Mg_{0.03}\square_{0.44}O_4$ and $Fe^{3+}_{2.59}Ti_{0.01}V_{0.03}Al_{0.04}\square_{0.33}O_4$, respectively. These compositions strongly contrast with those obtained for the Ti-bearing spinels included in the surrounding outcrops of mafic cumulates and olivine leucogabbros, which follow closely the ideal ulvöspinel–magnetite solid solution and show generally distinct oxidation-induced exsolution (Fig. 6; Jesus 2002).

EPMA data and subsequent calculation of cation distributions assuming stoichiometry show that ilmenite in the massive oxide bodies has an atomic ratio Fe/Ti in the range 0.92 – 0.80 (Fig. 7). Magnesium contents are relatively high, ranging from 0.17 to 0.19 *apfu*, and those of Fe^{3+} can be as high as 0.15 *apfu*; V contents are

TABLE 2. REPRESENTATIVE EPMA RESULTS FOR SPINEL (A-Spl AND B-Spl TYPES) AND ILMENITE GRAINS MAKING UP THE ODIVELAS OREBODIES

	A-Spl (N = 3, n = 13)			B-Spl (N = 3, n = 11)			Ilm (N = 3, n = 12)		
Al_2O_3 wt%	3.77	0.59	(0.57-3.91)	0.90	0.76	(0.12-2.37)	0.03	0.07	(0.02-0.07)
MgO	2.13	0.06	(0.00-2.13)	0.08	0.02	(0.01-0.13)	4.83	5.04	(4.56-5.40)
MnO	0.41	0.00	(0.00-0.46)	0.00	0.05	(0.00-0.05)	0.67	0.70	(0.61-0.73)
V_2O_3	1.52	1.50	(0.73-1.52)	0.01	2.71	(0.01-2.71)	1.93	2.58	(1.85-2.58)
TiO_2	14.80	17.47	(5.59-20.17)	0.01	0.03	(0.00-0.76)	51.21	52.14	(50.73-52.67)
ZnO	0.09	0.01	(0.00-0.10)	0.02	0.00	(0.00-0.09)	0.00	0.00	(0.00-0.04)
NiO	0.00	0.00	(0.00-0.02)	0.11	0.00	(0.00-0.19)	0.01	0.00	(0.00-0.02)
FeO	70.95	68.00	(68.00-78.80)	84.81	77.87	(77.87-90.06)	40.91	38.78	(37.65-41.96)
Cr_2O_3	0.10	0.09	(0.02-0.10)	0.01	0.09	(0.00-0.09)	0.02	0.05	(0.00-0.95)
Total	93.77	87.72	(85.60-93.77)	85.94	81.54	(79.94-90.36)	99.62	99.37	(98.43-101.31)
Al *apfu*	0.02	0.14		0.04	0.03		0.00	0.00	
Mg	0.00	0.10		0.00	0.00		0.18	0.18	
Mn	0.00	0.01		0.00	0.00		0.01	0.01	
V	0.04	0.04		0.00	0.08		0.04	0.05	
Ti	0.46	0.36		0.00	0.00		0.95	0.96	
Zn	0.00	0.00		0.00	0.00		0.00	0.00	
Ni	0.00	0.00		0.00	0.00		0.00	0.00	
Fe^{2+}	0.00	0.00		0.00	0.00		0.74	0.75	
Fe^{3+}	1.98	1.92		2.62	2.54		0.11	0.05	
Cr	0.00	0.00		0.00	0.00		0.00	0.00	
ΣR^{2+}	0.00	0.12		0.01	0.00				
ΣR^{3+}	2.05	2.11		2.66	2.66				
Σ cations	2.52	2.59		2.67	2.67		2.04	2.02	
vacancies	0.48	0.41		0.33	0.33				

Cation distribution in spinels was normalized to 4 atoms of oxygen per formula unit (*apfu*), assuming $\Sigma Fe = Fe^{3+}$. Cation proportions in ilmenite were computed on a basis of 3 atoms of oxygen, accepting a complete solid-solution between $FeTiO_3$ and Fe_2O_3 compositions. N = number of samples examined, n = number of analyses made. In all cases, fresh grains of A-Spl, B-Spl, and ilmenite were analyzed.

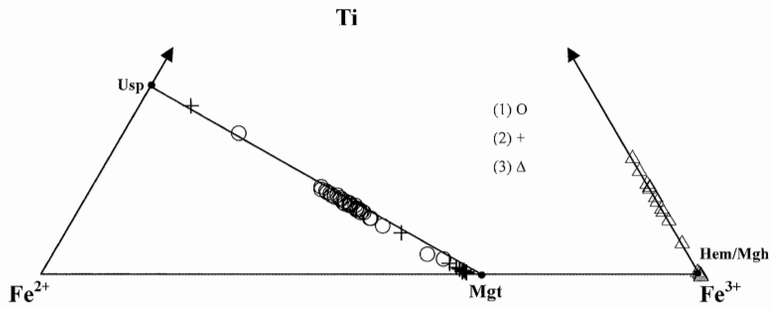

FIG. 6. Fe^{2+}–Fe^{3+}–Ti atom proportions in spinels of (1) mafic (oxide-rich) cumulates, (2) olivine leucogabbros, and (3) massive oxide bodies. Average chemical compositions of the former two groups are $Fe^{2+}_{1.28}Mg_{0.06}Mn_{0.01}Fe^{3+}_{1.10}V_{0.04}Ti_{0.34}Al_{0.17}O_4$ and $Fe^{2+}_{1.11}Mg_{0.01}Mn_{0.01}Fe^{3+}_{1.72}V_{0.04}Ti_{0.09}Al_{0.04}O_4$, respectively, considering all the available EPMA data (34 and 16 analyses, following the same order) and assuming the ideal stoichiometry of titanian magnetite in calculations (Jesus 2002).

quite uniform, ranging from 0.04 to 0.05 *apfu*. Averaging the values for all the available analyses, the formula $Fe^{2+}_{0.74}Mg_{0.18}Mn_{0.01}Fe^{3+}_{0.08}V_{0.04}Ti_{0.96}O_3$ is obtained, corresponding to an average ratio $(Fe^{3+})/\Sigma Fe \approx 9.8\%$. This chemical signature differs from that of ilmenite found in the surrounding outcrops of mafic cumulates and olivine leucogabbros (Fig. 7). We conclude that: 1) the Mg (and Mn) contents discriminate well the three groups of analyses, and seem to record the extent of chemical (re-)equilibration with the surrounding silicates (Mg becoming substantially higher where the silicates are not present), and 2) the amplitude of Fe^{3+} variation is quite independent of the rock type, although the analyses recorded for mafic cumulates and leucogabbros correspond to ilmenite grains with abundant hematite lamellae (Jesus 2002).

TABLE 3. MICRO-PIXE RESULTS OBTAINED FROM EACH OF THE TWO SPOTS ANALYZED IN A-Spl AND B-Spl GRAINS

	A-Spl, spot 1	A-Spl, spot 2	B-Spl, spot 1	B-Spl, spot 2
Ca	1190 ± 70	1030 ± 80	430 ± 40	160 ± 60
Ti	*9.4 ± 0.1*	*12.3 ± 0.1*	370 ± 40	270 ± 50
V	6260 ± 250	7000 ± 350	130 ± 20	< 40
Cr	550 ± 50	650 ± 70	100 ± 20	70 ± 30
Mn	600 ± 70	440 ± 90	490 ± 50	650 ± 70
Fe	*50.4 ± 0.6*	*64.8 ± 0.6*	72.9 ± 0.7	71.8 ± 0.7
Ni	< 130	< 130	230 ± 40	240 ± 50
Cu	< 45	270 ± 40	480 ± 40	380 ± 40
Zn	100 ± 30	120 ± 40	< 60	< 60

All values are in μg/g except those in italics, which are in wt%. The reported errors account only for the spectrum-counting statistics and fitting-error procedure. Values shown with a < are below the value stated, which represents the detection limit.

Micro-PIXE analysis

The possibility of spinel and ilmenite grains showing very fine-scale zonation was tested using micro-PIXE analyses of representative areas of the polished thin sections. Selected examples of the elemental mapping obtained for key metals (Fe, Ti and V) are shown in Figures 3 (E to L) and 8. Typical spectra of A–Spl and B–Spl obtained by micro-PIXE point analysis can be found in Figure 9; white circles in Figures 3E and 3F indicate the spots chosen to perform the point analyses.

It is quite straightforward to obtain Fe and Ti distribution maps from this type of sample, but imaging the distribution of vanadium presents some difficulties, owing not only to its lower contents, but especially to the proximity of V*K*α and Ti*K*β energy lines, which makes it impossible to map V distribution with the V*K*α energy line in titaniferous mineral phases. Although the V*K*β line has a much lower intensity (V*K*α/V*K*β intensity ratio is close to 8), it is almost free of interferences, as can be ascertained from the spectra shown in Figure 7. Using the V*K*β line and increasing the beam current to 500–600 pA at the expense of a small degradation in spatial resolution of the beam (~8–10 μm), a V-distribution map with a reasonable contrast can be obtained after 30 minutes of irradiation time (Fig. 8).

Information can be directly extracted from the maps obtained; they show that iron and titanium distributions are quite uniform (agreeing with available EPMA data) and distinct enough to discriminate clearly all the Fe–Ti oxides forming the massive bodies under study. Vanadium is shown to be mainly partitioned in A–Spl grains. The late hematite–goethite fracture infillings are clearly recognizable in the micro-PIXE imaging, because of their particular morphology and because they only contain iron, giving a stronger PIXE signal than the B–Spl spinel for this metal.

Two spots on A–Spl and B–Spl were chosen for micro-PIXE quantitative analysis; the results obtained

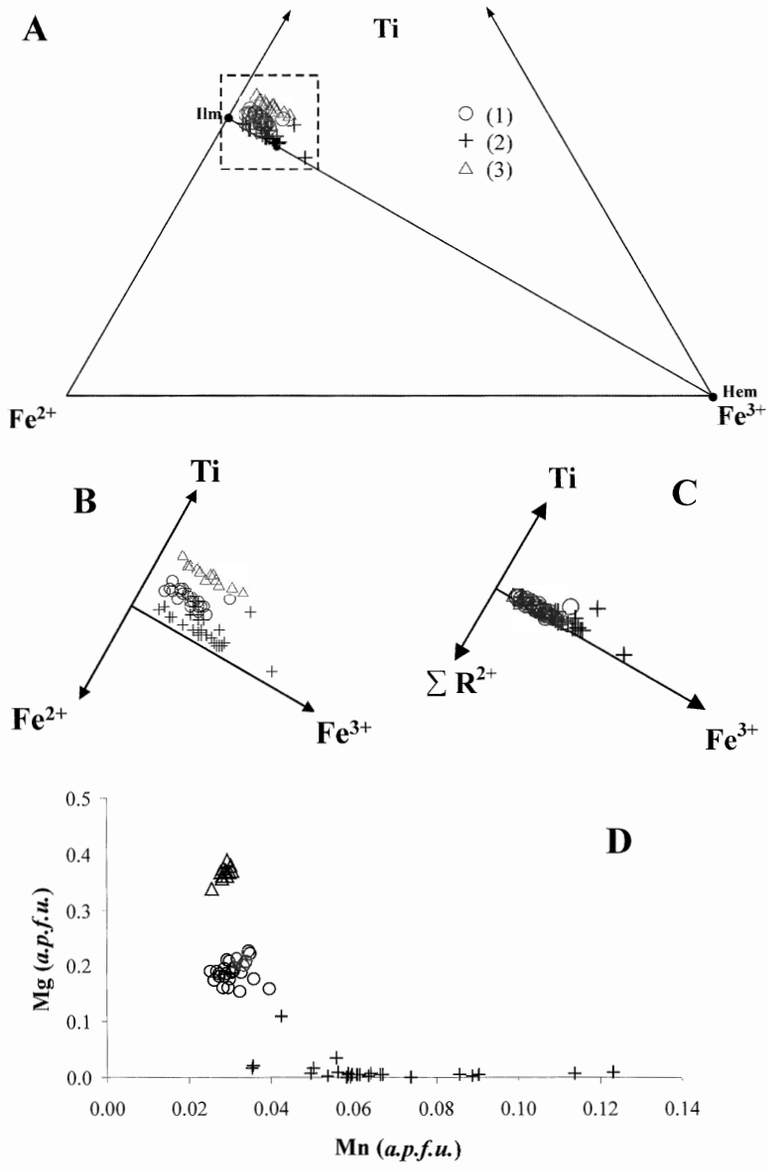

FIG. 7. A. Fe^{2+}–Fe^{3+}–Ti atom proportions in ilmenite of (1) mafic (oxide-rich) cumulates, (2) olivine leucogabbro, and (3) massive oxide bodies. B and C. Expanded-scale plots of A considering only the Fe^{2+} cations or the total of divalent cations (ΣR^{2+}), respectively; note that the three data points outside the consistent trend document crystal domains adjoining hematite lamellae. D. Distribution of the Mg and Mn contents in the ilmenite. Average chemical compositions of ilmenite in mafic cumulates and olivine leucogabbro are $Fe^{2+}_{0.83}Mg_{0.09}Mn_{0.02}Fe^{3+}_{0.08}V_{0.04}Ti_{0.96}O_3$ and $Fe^{2+}_{0.88}Mg_{0.01}Mn_{0.03}Fe^{3+}_{0.13}V_{0.05}Ti_{0.94}O_3$, respectively, taking all the available EPMA data (25 and 21 analyses, following the same order) and assuming the ideal stoichiometry of this oxide in the calculations (Jesus 2002).

TABLE 4. WHOLE-ROCK CHEMICAL COMPOSITION OF MASSIVE OXIDE BODIES

		INAA data					ICP–MS data		
	Units	ODV-5-A-1	ODV-5-A-2	ODV-5-4		Units	ODV-5-A-1	ODV-5-A-2	ODV-5-4
Au	ppb	<2	<2	<2	Ag	ppm	<0.3	<0.3	<0.3
Ag	ppm	<5	<5	<5	Cd	ppm	2.1	3.1	2.7
As	ppm	<0.5	<0.5	<0.5	Cu	ppm	593	131	265
Ba	ppm	<50	150	150	Mn	ppm	3912	1041	651
Br	ppm	<0.5	<0.5	<0.5	Mo	ppm	3	2	1
Ca	%	<1	<1	<1	Ni	ppm	78	10	21
Co	ppm	141	29	29	Pb	ppm	<3	33	30
Cr	ppm	318	263	63	Zn	ppm	491	25	61
Cs	ppm	<1	1	<1	Al	%	1.04	0.79	0.94
Fe (1)	%	42.9	43.1	49	Be	ppm	2	2	3
Hf	ppm	1	2	<1	Bi	ppm	<2	<2	<2
Ir	ppb	<5	<5	<5	Ca	%	<0.01	0.03	0.05
Mo	ppm	<1	<1	<1	K	%	0.01	<0.01	<0.01
Na	%	0.01	0.02	0.03	Mg	%	0.70	0.41	0.19
Ni	ppm	135	<42	<43	P	%	0.004	<0.001	<0.001
Se	ppm	<3	<3	<3	Sr	ppm	13	17	21
Ta	ppm	1.2	<0.5	<0.5	Ti	%	5.89	6.03	3.84
Th	ppm	<0.2	<0.2	<0.2	V	ppm	3514	3750	5520
Zn	ppm	558	75	98	Y	ppm	<1	<1	<1
					S	%	0.018	0.040	0.079
					Ge	ppm	0.9	0.9	1.6
					Se	ppm	5.2	6.1	5.0
					In	ppm	<0.2	<0.2	<0.2
					Sn	ppm	<1	1	<1
					Te	ppm	0.2	0.2	0.1
					Tl	ppm	<0.1	0.2	<0.1
					Bi	ppm	3.0	2.7	2.1
					FeO (2)	%	7.03	3.68	1.44
					Fe_2O_3/FeO (3)		7.61	15.63	47.54

(1) Total iron content, (2) FeO concentrations measured by titration, and (3) computed Fe_2O_3/FeO value.

are displayed in Table 3. The errors shown in this table are those reported by the GUPIX program, which only accounts for counting statistics and spectrum-fitting error. Error and inaccuracy in the determination of detector efficiency in charge-collection measurements are not accounted for, although they are expected to contribute 10% error to the analysis. The calculations indicate that A–Spl has a reasonably uniform concentration of V, with a value around 6500 μg/g, which is within the range of values measured with EPMA. V concentration in B–Spl was evaluated to be 130 μg/g in one of the points analyzed and below the detection limit of 40 μg/g in the other measured spot, indicating a significant variability that is also consistent with the available EPMA data. Concentrations of calcium can be ascribed to the late (supergene) precipitation of fine-grained carbonate in microcavities.

Whole-rock geochemistry

The whole-rock analysis of the massive oxide bodies (Table 4) reveals that up to 80% of their mass corresponds to Fe_2O_3, TiO_2, FeO and Al_2O_3, which is compatible with the petrographic and mineral-composition data reported above. Table 4 also shows that values of the ratio Fe_2O_3/FeO are extremely high, recording quite well the large amounts of (titanian) maghemite observed in the samples studied. The FeO concentrations appear thus to reflect exclusively the presence of ilmenite. Indeed, considering the modal proportions of

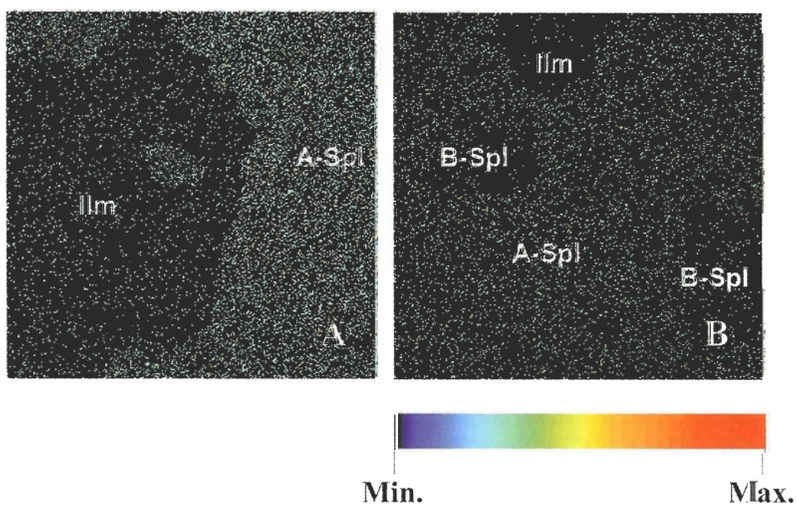

FIG. 8. Micro-PIXE images of vanadium distribution over the same areas as in Figures 3E (A) and 3F (B) using the V*K*β line. Maps were obtained from a 2640 × 2640 μm² scan area; white dots on Figures 3E and 3F represent the spots selected for micro-PIXE point analyses.

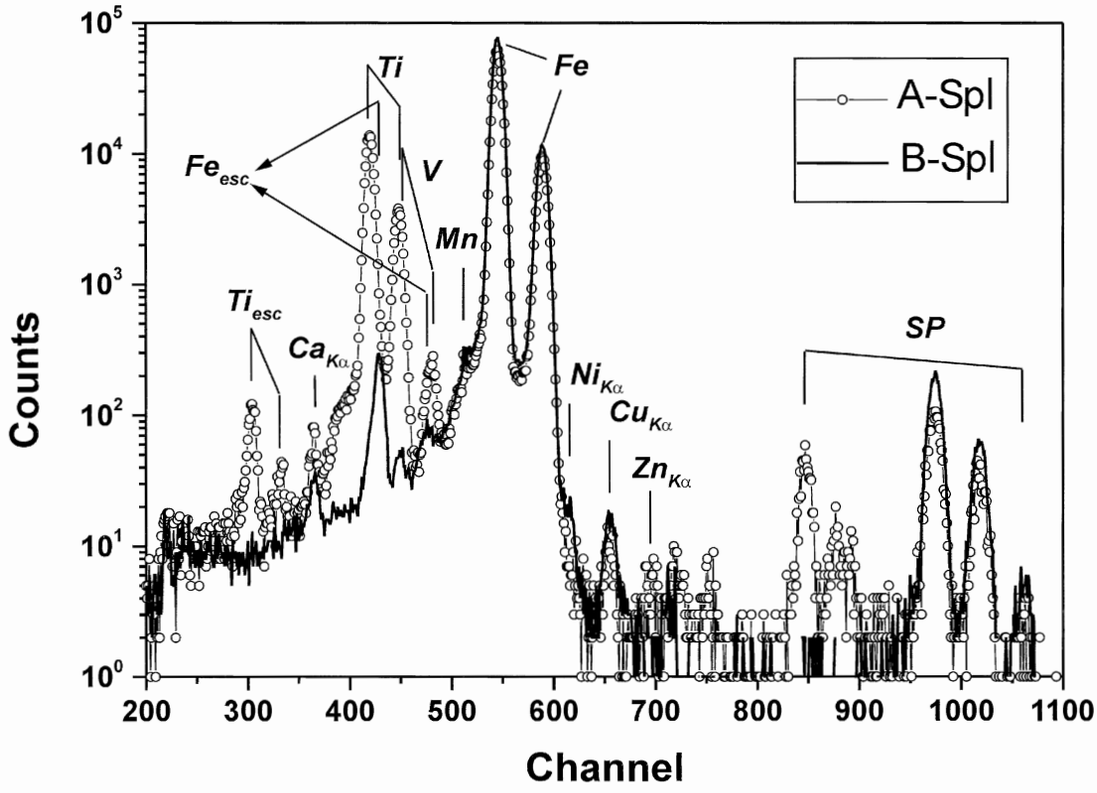

FIG. 9. Typical micro-PIXE spectra obtained from point analysis on A–Spl and B–Spl grains. Apart from the *K* X-ray lines (*K*α and *K*β or just the *K*α line) of Ca, Ti, V, Mn, Fe, Ni, Cu and Zn, the escape peaks (esc) of Ti and Fe, and the region of the spectrum with sum peaks (SP) are also indicated. As Cr*K*α has almost the same energy as the V*K*β line, and the Cr*K*β has almost the same energy as the Mn*K*α line, Cr*K* X-ray lines are not indicated in the spectra, and they can only be resolved as a result of a spectrum-fitting procedure. White dots on Figures 3E and 3F represent the spots selected to perform point analyses.

all the mineral phases in each sample, their density (as reported by Carmichael 1990), and the average Fe^{2+} content of ilmenite, differences between the calculated and the experimental bulk FeO values do not exceed 5%, the variations being ascribable to primary heterogeneity in the distributions of oxide minerals. Greater deviations are obtained for weathered samples (like ODV–5–4 in Table 4), certainly due to significant and variable increase of rock porosity, as observed, thus leading to uncertainties in the calculation of the volumes occupied by the different oxides and hydroxides.

A similar reasoning suggests that the chemical nature and the relative abundance of the main oxide minerals justify the extent of the variation obtained for the Al, Mg, Mn, Ti and V whole-rock contents. The measured concentrations in Cr, Ni and Co suggest also that the observed spinels do contain trace amounts of these metals. The presence of Cr and Ni was confirmed by micro-PIXE analysis (Fig. 9).

DISCUSSION

The results we obtained show unequivocally that both A–Spl and B–Spl must be titanian maghemite and maghemite, respectively. In fact, both show all petrographic characteristics of a spinel-group mineral, their XRD powder pattern corresponds to that of a spinel with an *a* value similar to the one published for maghemite, EPMA and Mössbauer fail to show any Fe^{2+} in them, and the Mössbauer hyperfine parameters are also similar to those normally ascribed to this mineral.

The Odivelas orebodies raise several questions that need explanation, most notably the origin of the oxide aggregates themselves and the striking difference in oxidation state between them and the surrounding country-rocks.

Generally speaking, the formation of maghemite is considered to result from the supergene alteration of magnetite or titanian magnetite, under such conditions

that structural conversion to hematite (or hematite ± ilmenite) or precipitation of iron hydroxides is inhibited. As far as we know, there are no references to hypogene, let alone primary, maghemite or titanian maghemite in igneous bodies. Since maghemite is invariably metastable with respect to hematite (*e.g.*, Waychunas 1991), primary crystallization of the former would imply a considerable kinetic barrier to hematite crystallization, a situation difficult to envisage for such a simple ionic structure. The same applies to the total oxidation of iron in magnetite or titanian magnetite at temperatures anywhere near the solidus: conversion to hematite ± ilmenite is to be expected, and was indeed found for temperatures higher than ~600°C in the experimental investigations reported and cited in Banerjee (1991). Accordingly, the maghemitic bodies of Odivelas must result from secondary alteration of titanian magnetite accumulations at temperatures much lower than the magmatic ones. However, it is very unlikely that the oxidation leading to maghemite formation is supergene. In fact, the ore is extremely coarse-grained and anhydrous, suggesting annealing at relatively high temperatures, and the supergene alteration they show is represented by rather abundant hematite ± goethite aggregates that cut (as late, generally polyphase veins) or otherwise alter the older crystals of maghemite. There is some further circumstantial evidence of high temperatures of oxidation in the form of a total absence of chemical gradients from rim to core in the spinel grains, although this absence may, in principle, also result from a very long process of oxidation at lower temperatures, in the absence of H_2O.

The chemical composition of the maghemite crystals, with some titanium, aluminum and magnesium, points to titanian magnetite as the parent mineral phase; titanian magnetite and ilmenite, in some cases with exsolved hematite, are also the only oxide phases present in the surrounding gabbroic rocks. Accumulations of magnetite crystals in layered gabbros are well known and normally result from the settling of crystals during the evolution of the magmatic chambers. At Odivelas, such accumulations have not been found, but gabbro layers and ultramafic cumulate lenses very rich in titanian magnetite do occur within the lower group of Series I, the same group that hosts the oxide bodies under study. Elsewhere in BIC, some 15 km from Odivelas, centimetric layers consisting almost exclusively of magnetic oxide minerals have recently been discovered, thus showing that BIC evolution did involve stages where settling of oxide grains took place with little codeposition of silicate phases. The Odivelas oxide bodies, however, are not stratiform, have irregular shapes, are of limited extent, and seem to lie almost at right angles to the regional layering. Normal settling in a magma chamber cannot produce these features. Some form of localized settling or strong reworking of older layers of oxide must have been in operation to form the accumulations observed at present. Localized settling will result wherever the distribution of crystals in the melt is not homogeneous. Two mechanisms may be responsible for the formation of such inhomogeneities: vortices associated to turbulence caused by the injection of magma plumes in a quiet magma chamber where extensive crystallization of oxides had already taken place (a highly probable occurrence owing to the synorogenic character of BIC), and clustering together of oxide grains due to the lower surface energy of spinel–spinel (as compared to spinel–silicate) contacts, which would favor the segregation of oxide grains from oxide–silicate mixtures (Boudreau & McBirney 1997). Reworking of previous accumulations of oxide is also to be expected, especially if the floor of the magma chamber consisted of unconsolidated accumulations of crystals derived from the magma. The Odivelas oxide bodies are embedded in layered primitive gabbroic to ultramafic rocks, which have a (much) lower density than magnetite or titanian magnetite. As the magma chamber floor needs not be horizontal and the syntectonic character of the BIC makes tectonic disturbance of the magma chamber a likely event during all stages of emplacement and consolidation, the stage is set for gravity instability of former lenticular bodies of spinel, resulting in their sliding down-slope and in their sinking downward through the unconsolidated accumulations of the earlier silicate minerals.

The wallrock outcrops nearest to the oxide bodies of Odivelas were unaffected by the total oxidation of titanian magnetite to titanian maghemite recorded in the oxide bodies; ilmenite included mostly as oikocrystic grains within the oxide bodies were also unaffected. In the present state of outcrop conditions, it is not possible to determine whether there is an oxidation gradient between the oxide bodies and the surrounding country-rocks, or whether the oxidation observed resulted from some kind of (unknown) special process that affects exclusively the accumulated spinels (?). Assuming that such a "special process" does not exist, the extreme spatial confinement of the oxidation process invites an explanation. As stated above, this process seems to have occurred at relatively high temperatures, which means that it should have resulted from the percolation of oxidizing fluids known to be efficiently produced in the final stages of magmatic cooling of the gabbroic suite (Mathez 1984). Evidence for the percolation of any fluids besides those responsible for the late supergene alteration is absent within the oxide bodies and in the rocks immediately surrounding them, but this absence may be an artifact of poor exposure and a general recrystallization of the spinels, which obliterated any prior structures and textures that may have been present. Indeed, at other places in the complex, most importantly in the vicinity of shear zones, evidence can be found for the circulation of late fluids, resulting in heterogeneous, and in some cases extensive, "retrogression" of the gabbros, with neoformation of amphiboles and phyllosilicates. Such assemblages of secondary minerals

document a high activity of H_2O. Thus, fluid circulation did occur in the late phases of BIC evolution but, apart from the obviously supergene phenomena already referred to (*e.g.*, hematite–goethite fracture infillings), no hydrated minerals whatsoever can be found within the oxide bodies, even in trace amounts. The limitation of the oxidizing event to the oxide bodies may be due to rheological differences between them and the host rocks, which would promote the concentration of fissures at their (now hidden) mutual contacts. Intergranular diffusion through spinel–spinel contacts would then ensure the oxidation of the entire accumulations of spinel, but leave the spinel grains disseminated in the surrounding rocks untouched, owing to the intervening silicate grains; in the absence of H_2O, the latter also would show no alteration, owing to the great sluggishness of silicate reactions at temperatures below ~600°C. The lack of structural inversion to a hematite-like structure may have been assisted by the presence of Al (Bannerjee 1991) and V in the original titanian magnetite.

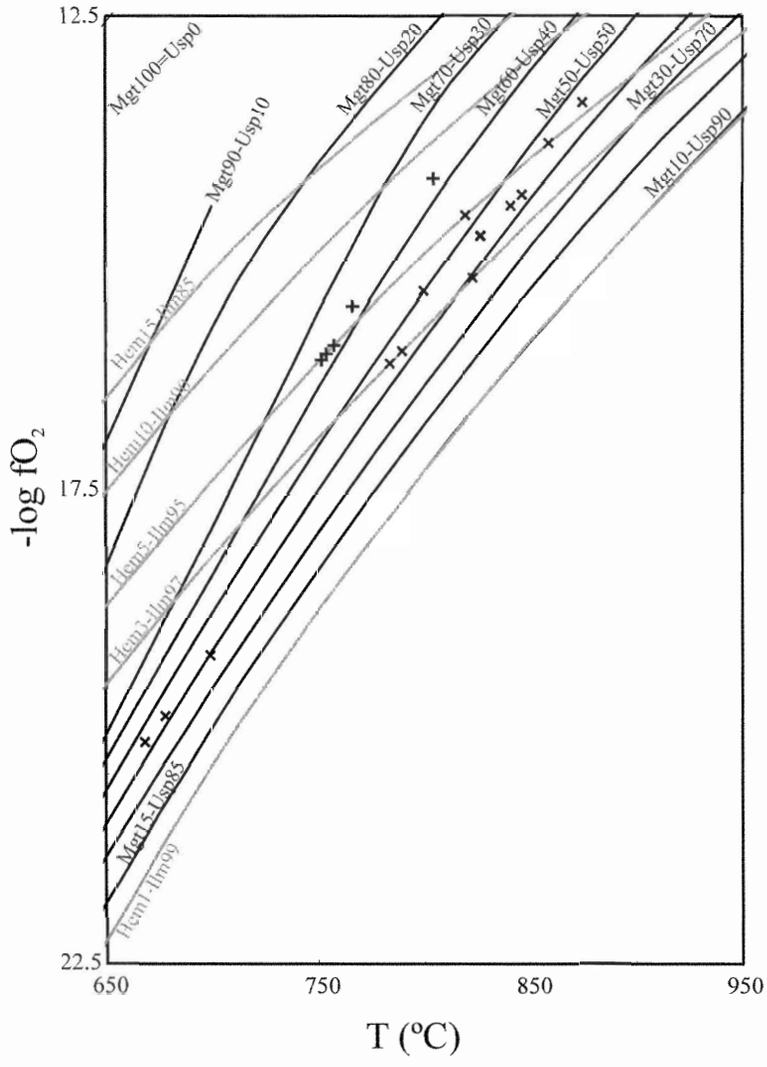

FIG. 10. Temperature and $f(O_2)$ estimates following the model of Buddington & Lindsley (1964), using the available EPMA data for spinel and ilmenite grains included in gabbroic rocks belonging to the lower group of Series I at Odivelas.

It should be noted that calculations made by the method of Buddington & Lindsley (1964) using the chemical compositions determined by EPMA, indicate that the oxide assemblages included in the gabbroic country rocks of Odivelas ceased to re-equilibrate at temperatures between 650 and 675°C and log oxygen fugacities around –20 (Fig. 10). Maghemite formation thus seems to have taken place after chemical closure of the oxide assemblages in the gabbros and is, indeed, dependent on the localized circulation of oxidizing fluids.

The presence of ilmenite and a Ti-poor spinel (B–Spl) coexisting with the titanian maghemite (A–Spl) in the oxide bodies of Odivelas needs also a plausible geochemical explanation. A significant part of the observed ilmenite should have resulted from coprecipitation with the original titanian magnetite. Indeed, the chemical signature of the ilmenite present in the oxide-rich cumulate lenses included in the surrounding country-rocks shows some similarities with the ilmenite in the oxide bodies; as a matter of fact, the latter even presents higher Mg contents, probably reflecting the scarcity of silicate mineral phases in the ores. However, we cannot rule out the possibility that some of the ilmenite in the oxide bodies at Odivelas formed as a product of early oxidation of the primary titanian magnetite, following the general equation (Buddington & Lindsley 1964):

$$6Fe_2TiO_4 + O_2 = 6FeTiO_3 + 2Fe_3O_4$$
Usp in Mgt Ilm Mgt

which shifts to the right as temperature decreases and $f(O_2)$ rises. If complete, this reaction leads to magnetite close to Fe_3O_4 hosting more or less abundant ilmenite lamellae that can ultimately form external and discrete grains of ilmenite (for complementary data, see also, *e.g.*, Snyder *et al.* 1993, Pownceby & Fisher-White 1999). In the oxide-rich cumulates, the most similar equivalents to the orebodies before maghemite formation, exsolution of ilmenite lamellae occurs, but not as extensively as in the surrounding olivine leucogabbro, where oxide abundance is lower. Nevertheless, some subsolidus re-equilibration of the precursor titanian magnetite of the oxide bodies would be expected in the final magmatic stages of the system, particularly in the grains richer in Ti, where the chemical drive for exsolution is more effective. Therefore, such grains should rapidly reach a near-ideal composition of magnetite in accordance with the above-cited equation. The magmatic ilmenite could thus grow at the expense of ilmenite exsolved from the precursor spinel, a process that would also contribute to develop the currently observed poikilitic texture of the ilmenite grains. The near-ideal magnetite that results from this exsolution process would then oxidize to maghemite, thus explaining the present-day Ti-poor spinel phase (B–Spl), which still preserves some of its original chemical signature, namely its contents of V and, less extensively, Mg and Al. The low abundance of this Ti-poor spinel is easily explained by the stoichiometry of the reaction above, since six moles of titanian magnetite break down to a 3:1 (molar) aggregate of ilmenite and magnetite.

However, the ilmenite lamellae that this process would have produced are not observed (even as a product of replacement) in the Ti-rich spinel (A–Spl). This may well be a consequence of the strong oxidation later experienced by the oxide aggregate, which would have promoted the redistribution of Ti in A–Spl and so allowed the oxidation process to proceed beyond the normal limit in the proportion of vacancies in maghemite. The total absence of chemical gradients from rim to core in the spinel minerals provides further circumstantial evidence for high velocities of cation diffusion during this process of resorption of ilmenite lamellae; nevertheless, the possibility cannot be ruled out that the optically heterogeneous (but chemically uniform) cores that are in some cases observed in A–Spl (Fig. 3B) represent a subtle textural remnant of the former chemical heterogeneity of the titaniferous spinel grains. Such re-absorption processes cannot be expected in the spinel grains that had already reached their ideal magnetite composition because this would require inter-grain Ti diffusion; the Ti-poor spinel phase B–Spl would thus be preserved.

It is known that ilmenite can withstand total oxidation of accompanying titanian magnetite to titanian maghemite in lavas or hypabyssal rocks altered in near-surface conditions (Buddington & Lindsley 1964). In such contexts, ilmenite decomposes partially to rutile, anatase and secondary hematite; none of these products is found in the Odivelas bodies of oxide minerals. This absence is taken to indicate that at Odivelas, the oxidation to maghemite occurred at temperatures much higher than normal supergene conditions.

Conclusions

The Odivelas oxide bodies are composed of coarse polygonal titanian maghemite, poikilitic ilmenite and interstitial maghemite, locally partially weathered to hematite ± goethite. Mössbauer spectroscopy shows that all ferrous iron belongs to the ilmenite, *i.e.*, the spinel is ferrian. X-ray diffractometry demonstrates that the main oxide phases have the spinel structure; EPMA shows the spinels to be indeed titanian maghemite or maghemite, micro-PIXE reveals that there is no chemical zonation in either spinel or ilmenite, and whole-rock geochemistry shows the ratio ferrous/ferric iron to be consistent with mineral compositions and modal proportions.

The oxide bodies must have resulted from gravitational instability of spinel layers accumulated at the bottom of a gabbroic magma chamber, as shown by their irregular shape and angular relationships with the regional layering. Textural relationships and the total

absence of hydrated minerals indicate that maghemite formation is a hypogene process, which occurred after chemical closure of the oxide assemblages in the country rocks. Confinement of this oxidation process to the oxide bodies seems to be due to inter-grain diffusion and some sort of fluid conduction to the oxide bodies owing to rheological differences between them and the country rocks. Early processes of exsolution due to late magmatic oxidation generated some of the ilmenite along with precursor magnetite, the latter being subsequently oxidized to maghemite during the main oxidizing event. Incorporation of minor cations in maghemite could have stabilized it against structural inversion to hematite, and ilmenite remained stable during the oxidation of the spinel.

Acknowledgements

This work was supported by the Portuguese Agency "Fundação para a Ciência e Tecnologia" (FCT) through the research project 12/2.1/CTA/82/94 – PROGEREMIN. Ana Jesus acknowledges also the FCT, Ph.D. grant SFRH/BD/6355/2001. Comments by Drs. Eric Force and Robert F. Martin improved the original manuscript significantly.

References

Allan, J.E.M., Coey, J.M.D., Sanders, I.S., Schwertmann, U., Friedrich, G. & Wiechowski, A. (1989): An occurrence of a fully-oxidized natural titanomaghemite in basalt. *Mineral. Mag.* **53**, 299-304.

Alves, L.C., Breese, M.B.H., Alves, E., Paúl, A., Da Silva, M.R., Da Silva, M.F. & Soares, J.C. (2000): Micron-scale analysis of SiC/SiC_f composites using the new Lisbon Nuclear Microprobe. *Nucl. Instrum. Meth.* **B161-163**, 334-338.

Andrade, A.S. (1974): Sur l'âge des orthogneiss d'Alcáçovas (Alentejo) et des filons (basiques et acides) qui les recoupent. *Mem. Not. Museu Lab. Mineral. Geol. Univ. Coimbra* **78**, 29-36.

_____ (1983): *Contribution à l'analyse de la suture Hercynienne de Beja (Portugal), perspectives métallogéniques.* Thèse de doctorat, INLP, Univ. Nancy, Nancy, France.

Araújo, A. (1995): *Structure of a Geotransversal between Brinches and Mourão (Ossa–Morena Zone): Implications to the Geodynamic Evolution of the Southeast Margin of the Iberian Autochthon Terrain.* Ph.D. thesis, Univ. of Évora, Portugal (in Portuguese, with Engl. abstr.).

Banerjee, S.K. (1991): Magnetic properties of Fe–Ti oxides. *In* Oxide Minerals: Petrologic and Magnetic Significance (D.H. Lindsley, ed.). *Rev. Mineral.* **25**, 107-128.

Bayliss, P., Erd, R.C., Mrose, M., Roberts, A.C. & Sabina, A.P. (1993): *Mineral Powder Diffraction File Databook.* International Center for Diffraction Data, Park Lane, Pennsylvania.

Boudreau, A.E. & McBirney, A.R. (1997): The Skaergaard layered series. III. Non-dynamic layering. *J. Petrol.* **38**, 1003-1020.

Bowen, L.H., De Grave, E. & Vandenberghe, R.E. (1993): Mössbauer effect studies of magnetic soils and sediments. *In* Mössbauer Spectroscopy Applied to Magnetism and Materials Science **1** (G.J. Long & F. Grandjean, eds.). Plenum Press, New York, N.Y. (115-159).

Buddington, A.F. & Lindsley, D.H. (1964): Iron–titanium minerals and their synthetic equivalents. *J. Petrol.* **5**, 310-357.

Carmichael, R.S. (1990): *Practical Handbook of Physical Properties of Rocks and Minerals* (2nd ed.). CRC Press, Boston, Massachusetts.

Da Costa, G.M., De Grave, E., Bowen, L.H., De Bakker, P.M.A. & Vandenberghe, R.E. (1995): Temperature dependence of the hyperfine parameters of maghemite and Al-substituted maghemites. *Phys. Chem. Minerals* **22**, 178-185.

Dallmeyer, R.D., Fonseca, P.E., Quesada, C. & Ribeiro, A. (1993): $^{40}Ar/^{39}Ar$ mineral age constraints for the tectonothermal evolution of the Variscan Suture in southwest Iberia. *Tectonophysics* **222**, 177-194.

Duchesne, J.C. (1999): Fe–Ti deposits in Rogaland anorthosites (south Norway): geochemical characteristics and problems of interpretation. *Mineral. Deposita* **34**, 182-198.

Fonseca, P.E. (1995): *Study of the Variscan Suture in the Iberian SW, in the Serpa – Beja – Torrão and Alvito – Viana Regions.* Ph.D. thesis, Univ. of Lisbon, Lisbon, Portugal (in Portuguese, with Engl. abstr.).

_____ (1999): Geophysical prospecting through vertical components of the magnetic field in the Odivelas – Ferreira do Alentejo. Internal Report DPMM – IGM, Lisbon, Portugal (in Portuguese).

Frost, B.R. & Lindsley, D.H. (1991): Occurrence of iron–titanium oxides in igneous rocks. *In* Oxide Minerals: Petrologic and Magnetic Significance (D.H. Lindsley, ed.). *Rev. Mineral.* **25**, 433-468.

Gonçalves, M.A., Mateus, A. & Oliveira, V. (2001): Geochemical anomaly separation by multifractal modeling. *J. Geochem. Explor.* **72**, 91-114.

Grime, G.W. & Dawson, M. (1995): Recent developments in data acquisition and processing on the Oxford scanning proton microprobe. *Nucl. Instrum. Meth.* **B104**, 107-113.

Irvine, T.N. (1987): Glossary of terms for layered intrusions. *In* Origin of Igneous Layering (I. Parsons, ed.). D. Reidel Publishing Co., Dordrecht, The Netherlands (641-647).

JESUS, A.P. (2002): *Fe–Ti–V Mineralizations and Sulphide Occurrences in Gabbroic Rocks of the Beja Igneous Complex (Odivelas – Ferreira do Alentejo)*. M.Sc. thesis, Univ. of Lisbon (in Portuguese, with Engl. abstr.).

KÄRKKÄNNEN, N. & APPELQVIST, H. (1999): Genesis of a low grade apatite – ilmenite – magnetite deposit in the Kauhajärvi gabbro, western Finland. *Mineral. Deposita* **34**, 754-769.

MATEUS, A., JESUS, A.P., OLIVEIRA, V., GONÇALVES, M.A. & ROSA, C. (2001): Vanadiferous iron–titanium ores in gabbroic series of the Beja Igneous Complex (Odivelas, Portugal); remarks on their possible economic interest. *Est. Notas e Trabalhos I.G.M.* **43**, 3-16.

MATHEZ, E.A. (1984): Influence of degassing on oxidation states of basaltic magmas. *Nature* **310**, 371-375.

MAXWELL, J.A., TEESDALE, W.J. & CAMPBELL, J.L. (1995): The Guelph PIXE software package II. *Nucl. Instrum. Meth.* **B95**, 407-421.

MCBIRNEY, A.R. & NICOLAS, A. (1997): The Skaergaard layered series. II. Magmatic flow and dynamic layering. *J. Petrol.* **38**, 569-580.

PARSONS, I., ed. (1987): *Origin of Igneous Layering*. D. Reidel Publishing Co., Dordrecht, The Netherlands.

PERROUD, H., BONHOMMET, N. & RIBEIRO, A. (1985): Paleomagnetism of Late Paleozoic igneous rocks from southern Portugal. *Geophys. Res. Lett.* **12**, 45-48.

POWNCEBY, M.I. & FISHER-WHITE, M.J. (1999): Phase equilibria in the systems Fe_2O_3–MgO–TiO_2 and FeO–MgO–TiO_2 between 1173 and 1473 K, and Fe^{2+}–Mg mixing properties of ilmenite, ferrous-pseudobrookite and ulvöspinel solid solutions. *Contrib. Mineral. Petrol.* **135**, 198-211.

PUTNIS, A. (1992): *Introduction to Mineral Sciences*. Cambridge Univ. Press, Hampshire, U.K.

QUESADA, C., FONSECA, P.E., MUNHÁ, J.M., OLIVEIRA, J.T. & RIBEIRO, A. (1994): The Beja – Acebuches Ophiolite Complex (Southern Iberian Variscan Fold Belt): geological characterization and geodynamic significance. *Bol. Geol. y Minero* **105**, 3-49.

RAMDANI, A., STEINMETZ, J., GLEITZER, C., COEY, J.M.D. & FRIEDT, J.M. (1987): Perturbation de l'échange électronique rapide par des lacunes cationiques dans $Fe_{3-x}O_4$ ($x \leq 0.09$). *J. Phys. Chem. Solids* **48**, 217-228.

RUMBLE, D., III, ed. (1976): *Oxide Minerals*. Mineral Soc. Am., Short Courses Notes **3**.

SANTOS, J.F. (1990): *Petrology of the Western Sector of the Odivelas Unit (Beja Massif)*. M.Sc. thesis, Univ. of Aveiro, Aveiro, Portugal (in Portuguese, with Engl. abstr.).

_____, ANDRADE, S.A. & MUNHÁ, J. (1990): Variscan orogenic magmatism on the southern border of the Ossa Morena Zone. *Comun. Serv. Geol. Portugal* **76**, 91-124 (in Portuguese, with Engl. abstr.).

SILVA, J.M. (1945): Notes about the iron deposit of Odivelas. *Est. Notas e Trabalhos S.F.M.* **1**, 286-292 (in Portuguese).

SILVA, L.C., QUADRADO, R. & RIBEIRO, L. (1970): Previous notes about the existence of a zoned structure and of anorthosites in the gabbro–dioritic massif of Beja. *Bol. Mus. Lab. Min. Geol. Univ. Lisboa* **11**, 223-232 (in Portuguese, with Engl. abstr.).

SNYDER, D., CARMICHAEL, I.S.E. & WIEBE, R.A. (1993): Experimental study of liquid evolution in an Fe-rich layered mafic intrusion: constraints of Fe–Ti oxide precipitation on the T–fO_2 and T–ρ paths of tholeiitic magmas. *Contrib. Mineral. Petrol.* **113**, 73-86.

TOPPLIS, M.J. & CARROLL, M.R. (1995): An experimental study of the influence of oxygen fugacity on Fe–Ti oxide stability, phase relations, and mineral–melt equilibria in ferrobasaltic systems. *J. Petrol.* **36**, 1137-1170.

VANDENBERGHE, R.E., BARRERO, C.A., DA COSTA, G.M., VAN SAN, E. & DE GRAVE, E. (2000): Mössbauer characterization of iron oxides and (oxy)hydroxides: the present state of the art. *Hyperf. Interact.* **126**, 247-259.

_____, HUS, J.J. & DE GRAVE, E. (1998): Evidence from Mössbauer spectroscopy of neo-formation of magnetite/maghemite in the soils of loess/paleosol sequences in China. *Hyperf. Interact.* **117**, 359-369.

WAERENBORGH, J.C., FIGUEIRAS, J., MATEUS, A. & GONÇALVES, M. (2002): Nature and mechanism of ilmenite alteration: a Mössbauer and X-ray diffraction study of oxidized ilmenite from the Beja–Acebuches Ophiolite Complex (SE Portugal). *Mineral. Mag.* **66**, 421–430.

_____, FIGUEIREDO, M.O., CABRAL, J.M.P. & PEREIRA L.C.J. (1994): Powder XRD structure refinements and ^{57}Fe Mössbauer effect study of synthetic $Zn_{1-x}Fe_xAl_2O_4$ ($0 < x \leq 1$) spinels annealed at different temperatures. *Phys. Chem. Minerals* **21**, 460-468.

WAYCHUNAS, G.A. (1991): Crystal chemistry of oxides and oxyhydroxides. *In* Oxide Minerals: Petrologic and Magnetic Significance (D.H. Lindsley, ed.). *Rev. Mineral.* **25**, 11-68.

WEBER, H.P. & HAFNER, S.S. (1971): Vacancy distribution in nonstoichiometric magnetites. *Z. Kristallogr.* **133**, 327-340.

YOUNG, R.A., SAKTHIVEL, A., MOSS, T.S. & PAIVA-SANTOS, C.O. (1995): DBWS–9411 – an upgrade of the DBWS*.* programs for Rietveld refinement with PC and mainframe computers. *J. Appl. Crystallogr.* **28**, 366-367.

Received January 11, 2003, revised manuscript accepted September 26, 2003.